Resonance Raman Evidence for Multistate Contributions to the Lowest Optical Transitions of Azulenic−Thiobarbituric Acid Donor−Acceptor Chromophores

Weinan Leng,[†] C. H. Wang,[‡] Alfred E. Asato,[§] and Anne Myers Kelley*[,†]

Department of Chemistry, Kansas State University, Manhattan, Kansas 66506-3701, Department of Chemistry, University of Nebraska−Lincoln, Lincoln, Nebraska 68588-0304, Department of Physics, National Sun Yat-sen University, Kaohsiung, Taiwan 80424, and Department of Chemistry, University of Hawaii at Manoa, Honolulu, Hawaii 96822

Received: June 7, 2002

Resonance Raman spectra have been obtained for two electron donor−acceptor substituted "push−pull" conjugated molecules possessing guaiazulene donor groups and thiobarbituric acid acceptor groups. One of these was the subject of a recent detailed hyper-Rayleigh scattering excitation profile throughout the two-photon resonant region [Hsu, C.-C. ; Liu, S.; Wang, C. C.; Wang, C. H. Dispersion of the first hyperpolarizability of a strongly charge-transfer chromophore investigated by tunable wavelength hyper-Rayleigh scattering. *J. Chem. Phys.* **2001**, *114*, 7103−7108] and an effort to calculate this profile with a Kramers−Kronig technique based on the two-state model for the first hyperpolarizabilities of strongly charge-transfer molecules [Kelley, A. M. Frequency-dependent first hyperpolarizabilities from linear absorption spectra. *J. Opt. Soc. Am. B* **2002**, *19*, 1890−1900]. The resonance Raman spectra of both azulene donor molecules show strong dispersion in the relative intensities of Raman lines of similar frequency as the excitation is tuned across the absorption band. This suggests that the broad visible absorption band has significant contributions from more than one electronic transition, although the presence of more than one molecular species differing in charge distribution and/or conformation cannot be ruled out. These effects are not observed in a chromophore having julolidine instead of guaiazulene as the donor group.

Introduction

π-conjugated organic molecules having strong intramolecular charge-transfer electronic transitions often have large molecular first hyperpolarizabilities (β) and show promise as chromophores in polymer-based second-order nonlinear optical materials.[1−3] In these molecules the lowest-energy excited electronic state has both a large transition dipole moment to the ground state and a large permanent dipole moment. The general quantum-mechanical expression for β, which involves summations over all possible intermediate electronic states,[4,5] is assumed to be dominated by paths involving just these two electronic states. When all of the optical frequencies fall below any one- or two-photon resonances, the result is the now-standard two-level formula for β initially derived by Oudar and Chemla (OC).[6] The OC formula has recently been modified to account for details expected to become important on or near resonance, including the finite lifetime of the charge-transfer state, inhomogeneous broadening, and the vibronic structure of the electronic transition.[7−10]

Molecular first hyperpolarizabilities are generally measured via either electric field induced second harmonic generation (EFISH) or hyper-Rayleigh scattering (HRS) at a single incident frequency in the near-infrared, often near but usually below two-photon resonance. Most studies of the frequency dependence of β have utilized a rather limited frequency range entirely within the nonresonant or preresonant regime. Although this is the frequency range in which most practical $\chi^{(2)}$ based devices are designed to operate, the rather gentle and monotonic dependence of β on frequency in the preresonant region makes these measurements rather insensitive to the differences between theoretical models. To test the two-level model in general and its various refinements, it would be very helpful to have measurements of the molecular hyperpolarizability throughout the region of two-photon resonance, where strong variations with wavelength are expected. We are aware of only two such measurements for organic "push−pull" donor−acceptor substituted molecules: HRS profiles by Wang and co-workers on a guaiazulene donor/thiobarbituric acid acceptor chromophore (see inset of Figure 1),[11] and SHG profiles in a poled DANS (4-(dimethylamino)-4′-nitrostilbene) side chain polymer by Otomo et al.[12] One of us recently derived a new theoretical equation for the frequency dispersion of β, based on a Kramers−Kronig transform of the linear absorption spectrum, that automatically incorporates the homogeneous line width of the transition and its vibronic structure in a manner that is exact within the two-electronic-state model.[10] However, the HRS dispersion curves calculated for Wang's chromophore with this method showed poor agreement with experiment, suggesting that the two-level picture may be inadequate for this chromophore.

Breakdown of the two-electronic-state model in this chromophore would not be surprising. In most of the other push−pull chromophores studied for nonlinear optical applications, neither the donor group nor the acceptor group has any electronic transitions in the visible region of the spectrum. The strong absorption that results when the donor and acceptor are covalently linked through a conjugated bridge is then reasonably

* Corresponding author.
[†] Kansas State University.
[‡] University of Nebraska−Lincoln and National Sun Yat-sen University.
[§] University of Hawaii at Manoa.

10.1021/jp026263s CCC: $22.00
Published on Web 09/24/2002

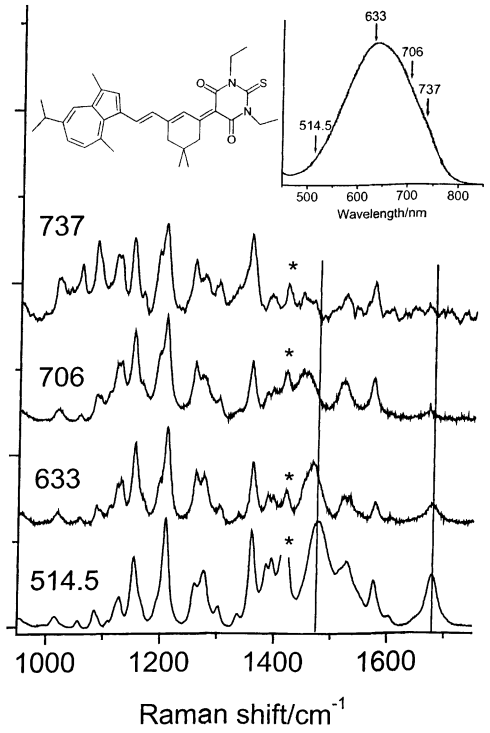

Figure 1. Resonance Raman spectra of 0.38 mM Chrom 2 in CH_2Cl_2 at the indicated excitation wavelengths. The asterisk marks a solvent line, truncated in some of the spectra. The inset shows the excitation wavelengths at various positions on the absorption spectrum in CH_2Cl_2. The two vertical lines through the Raman spectra mark bands that lose most of their intensity as the excitation wavelength is tuned to the red.

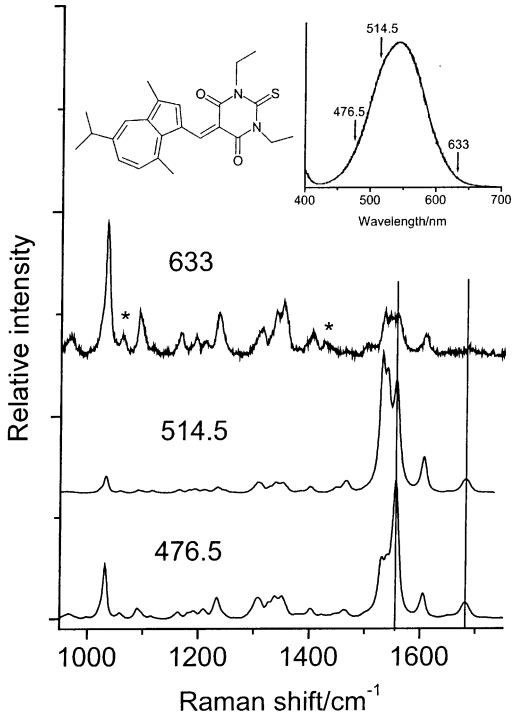

Figure 2. Same as Figure 1, for Chrom 4 (1.4 mM in CH_2Cl_2).

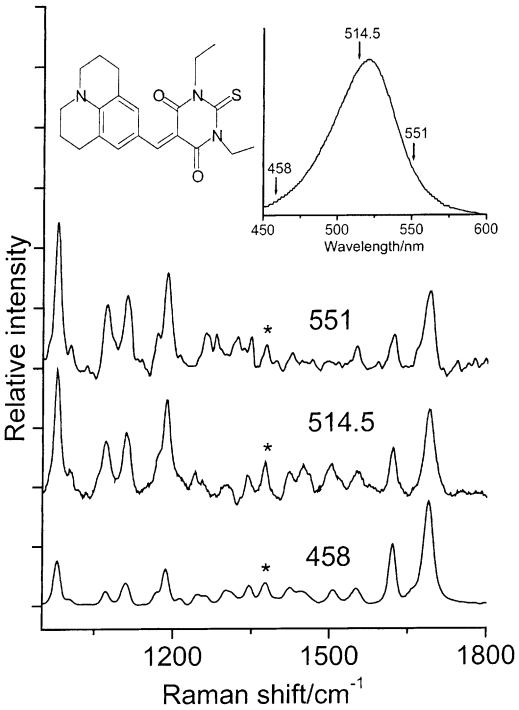

Figure 3. Same as Figure 1, for JTB in acetonitrile (concentrations vary with excitation wavelength).

interpreted as a charge-transfer excitation. In contrast, azulene and substituted azulenes all have an electronic absorption, albeit a weak one, in the same region of the visible spectrum as the putative charge-transfer band. It seems reasonable that two electronic states, one derived from the locally excited azulenic transition and the other from the charge-transfer excitation, both contribute to the strong visible absorption band. The locally excited state, which has an oscillator strength of only about 0.01 in azulene itself, may gain intensity by mixing with the charge-transfer transition in this low-symmetry system. If more than one electronic transition contributes significantly to the linear absorption spectrum and/or the first hyperpolarizability, the relationships between the two quantities derived in ref 10 are no longer expected to hold.

Resonance Raman spectra, excitation profiles, and depolarization ratios can be sensitive to the presence of multiple resonant states in several ways. In particular, if two electronic transitions having very different orbital characters are partially overlapping, one expects that the relative intensities of different vibrations will vary strongly as the excitation is tuned from the part of the absorption band where one state dominates to the part of the band where the other state dominates. Raman excitation profiles often have considerable structure (more than the absorption spectrum) even with a single resonant state, and fully interpreting that structure requires a detailed model for the electronic transition.[13,14] However, within the simple harmonic oscillator approximation the *relative* intensities of vibrations having similar frequencies are very similar when a single resonant electronic state is involved.[13] Large variations in the relative intensities of modes that are close in frequency but correspond to very different vibrational motions, are a good indication that more than one excited electronic state is involved. In addition, depolarization ratios that differ from 1/3 provide clear evidence for the contribution of more than one differently polarized electronic transition to the Raman enhancement.

In this paper, we apply resonance Raman spectroscopy to qualitatively evaluate the electronic state composition of the strong, broad visible absorption of the chromophore shown in Figure 1 (heretofore known as Chrom 2 as in the original paper reporting its HRS).[15] For comparison, we also present data on a related azulenic/thiobarbituric acid molecule, Chrom 4 (Figure 2), and another chromophore having the same thiobarbituric acid acceptor but with julolidine as the donor group (JTB, Figure 3). Julolidine itself does not absorb in the visible region of the

spectrum, and the solvent-dependent resonance Raman excitation profiles of JTB were previously analyzed successfully assuming a single resonant electronic state.[16]

Methods

Chrom 2 and Chrom 4 were synthesized as described previously.[15] Solutions for resonance Raman spectroscopy were prepared in CH_2Cl_2 at concentrations of 0.38 mM (Chrom 2) and 1.4 mM (Chrom 4). Excitation at 476.5 and 514.5 nm was obtained from a continuous wave (cw) argon-ion laser (Lexel model 95-4). Excitation at 633 nm was provided by a polarized He−Ne laser (Melles Griot). Excitation at 706 and 737 nm was provided by a Ti:sapphire laser (Spectra-Physics Tsunami) pumped by a frequency-doubled diode-pumped cw Nd:YVO_4 laser (Millenia Vs). The Ti:sapphire laser was designed to be used as a mode-locked picosecond laser but was operated without active mode-locking for this application, providing a narrower spectral bandwidth. Unwanted wavelengths were removed from the excitation source by passage through a grating prefilter (Ar^+), interference filter (He−Ne), or dispersing prism (Ti:sapphire) before being focused onto the sample contained in a rotating cell of about 2 mL volume. The Raman scattering was collected with reflective optics from the front face of the rotating cell in an approximately 135° backscattering geometry, passed through a polarization scrambler, dispersed with a Spex 1877 triple spectrograph, and detected with a Spex Spectrum One liquid nitrogen cooled CCD. Spectra were corrected for reabsorption and for the wavelength dependence of the collection and detection efficiency as described elsewhere.[14] Weak fluorescence backgrounds have also been subtracted from some spectra, although neither Chrom 2 nor Chrom 4 exhibited much fluorescence in the detection region of interest.

The resonance Raman spectra of JTB were obtained similarly as described in a previous publication.[16]

Resonance Raman depolarization ratios were measured by rotating a thin-film polarizer (Meadowlark Optics) placed before the polarization scrambler.

Geometry optimizations and vibrational frequency calculations were carried out using density functional theory (DFT) with the B3LYP exchange-correlation functional and the 6-31G basis set as implemented in Gaussian 98.[17] Semiempirical AM1 and MINDO3 calculations were also performed for comparison. The ZINDO semiempirical method as implemented in Gaussian 98 was used to generate electronic transition frequencies and transition dipole moments for each chromophore at the DFT and semiempirical ground-state equilibrium geometries. The ZINDO calculations included configuration interaction involving all single excitations from filled to virtual orbitals.

Results

Figures 1 and 2 show the resonance Raman spectra of Chrom 2 and Chrom 4, respectively, in CH_2Cl_2 at three or four excitation wavelengths ranging from the red side to the blue side of the absorption maximum. The excitation wavelengths used at various positions on the absorption bands are indicated on the insets. The absorption intensities for both compounds are very strong, with peak molar absorptivities of about 50 000 M^{-1} cm^{-1}.[15] Figure 3 shows comparable data for JTB in acetonitrile. JTB is moderately fluorescent, and even in a strongly Stokes-shifting solvent we could not obtain data of adequate quality with excitation to the red of 551 nm. For Chrom 2, excitation to the red of 737 nm was not attempted because of the declining collection and detection efficiency of our instrument beyond 850 nm.

All of the observed Raman lines of both Chrom 2 and Chrom 4 have depolarization ratios that are within experimental uncertainty of 1/3 at 476.5, 514.5, and 632.8 nm. The polarization data provide no evidence for contributions from more than one differently polarized electronic transition to any of the resonance Raman lines.

The spectra of Chrom 2 show more strong lines in the 1100−1300 cm^{-1} region than do the spectra of Chrom 4, suggesting that much of the intensity in this region arises from the cyclohexenyl ring and/or the additional polyenic double bond that differentiates the two structures. With the exception of two lines, the general appearance of the Chrom 2 resonance Raman spectra is similar at all excitation wavelengths. The increase in the relative intensities of most lower frequency lines at the reddest excitation is not necessarily significant; the excitation profiles of lower frequency lines generally peak at longer wavelengths than do the profiles for higher frequency lines for simple Franck−Condon overlap reasons.[13] However, the same considerations also show that the relative intensities of lines of similar frequency should not vary strongly with excitation wavelength.[13] In contrast, two vibrations of Chrom 2 that are fairly strong when excited at 514.5 or 633 nm exhibit a precipitous decline of intensity relative to other nearby lines as the excitation is tuned to the red. These two features are at ∼1480 and 1678 cm^{-1}, as indicated by the vertical lines in Figure 1. Both of these modes also appear to decrease in frequency somewhat as the excitation is tuned toward the red, although this may simply be a result of overlap with a lower frequency line that retains its intensity while the other line disappears. It is clear that there are a number of overlapping Raman transitions in the 1440−1490 cm^{-1} range.

Chrom 4 exhibits similar intensity patterns. The line at 1681 cm^{-1}, which corresponds to the 1678 cm^{-1} line of Chrom 2 (see below), decreases dramatically in intensity relative to nearby lines as the excitation is tuned to the red. The line at 1556 cm^{-1} also loses relative intensity although less dramatically, analogous to the 1480 cm^{-1} line of Chrom 2. The apparent changes in frequency observed in Chrom 2 are not seen in Chrom 4.

Chrom 2 in CH_2Cl_2 decomposes slowly (time constant of a few days) when exposed to room light to form a product that lacks the strong visible charge-transfer absorption band. Similar behavior was previously reported in chloroform.[15] We do not believe that these decomposition products, which will not be resonantly enhanced with visible excitation, influence our qualitative resonance Raman spectra. The resonance Raman spectra of Chrom 2 in acetonitrile, a solvent in which these absorption spectral changes are not observed, are nearly identical to those obtained in methylene chloride. In addition, Chrom 4 does not undergo evident decomposition in methylene chloride but exhibits the same wavelength-dependent Raman intensity pattern as Chrom 2.

JTB contains the same thiobarbituric acid acceptor group as the other two chromophores, but the guaiazulene donor is replaced by julolidine. Figure 3 shows that although the lower frequency lines do have greater relative intensities with redder excitation, there are no dramatic changes in the intensities of strong lines as seen in the other two molecules. In particular, the line at 1689 cm^{-1}, analogous to the 1678 and 1681 cm^{-1} lines of Chrom 4 and Chrom 2, retains a fairly constant intensity relative to other nearby lines as the excitation frequency is changed.

MINDO3 and AM1 vibrational normal mode calculations predict that the highest-frequency mode (apart from CH stretches) in all three molecules is primarily the symmetric

TABLE 1: Calculated (DFT B3LYP/6-31G) and Experimental Vibrational Frequencies[a]

	Chrom 2		Chrom 4		JTB		azulene	
mode description	expt	calc	expt	calc	expt[b]	calc	expt[c]	calc
sym C═O str	1678	1653	1681	1680	1689	1684		
asym C═O str		1631		1640		1642		
ethylenic C═C str.		1643						
azulene ring str (a_1)	1603	1619	1606	1618			1578	1660
cyclohexene C═C str	1522	1579						
azulene ring str (b_2)		1670		1668			1586	1665
azulene ring str (b_2)	1531	1586	1530	1588			1476	1555
C═C str of TBA link	1480	1505	1556	1568	1506	1496		
julolidine quinoidal str					1622	1672		
azulene ring str (a_1)	1575	1606	1539	1599			1534	1606
julolidine ring str					1552	1588		

[a] TBA = thiobarbituric acid (acceptor group). Symmetries given for the azulene modes refer to unsubstituted azulene only. [b] Reference 16. [c] Reference 18.

combination of the C═O stretches on the thiobarbituric acid acceptor group. DFT(B3LYP/6-31G) calculations give the symmetric C═O stretch as the highest frequency mode in Chrom 4 and JTB, in agreement with previous density functional theory calculations on JTB that used a larger basis set (6-311G**).[16] The DFT calculations place the symmetric C═O stretch considerably lower in frequency and below one of the azulene-localized vibrations in Chrom 2. We nevertheless believe that the 1678 and 1681 cm^{-1} modes of Chrom 2 and Chrom 4, which lose intensity dramatically with red excitation, correspond to roughly the same acceptor-localized normal mode as the 1689 cm^{-1} mode of JTB, which shows no such intensity anomaly. The other lines showing excitation wavelength-dependent intensities, the ~1480 cm^{-1} band of Chrom 2 and the 1556 cm^{-1} line of Chrom 4, are not as straightforwardly assigned, but the vibrational calculations suggest that they involve predominantly the C═C stretch adjacent to the thiobarbituric acid group, calculated to shift down by 63 cm^{-1} between Chrom 4 and Chrom 2. Table 1 summarizes the experimental and calculated (DFT) vibrational frequencies for all three chromophores in the 1470−1700 cm^{-1} region and also gives the experimental and calculated frequencies of unsubstituted azulene for comparison. The vibrational assignments of all lines except the symmetric C═O stretch must be considered quite tentative.

Table 2 presents the results of ZINDO calculations of the electronic excitations at the DFT ground-state geometry. In JTB, the ZINDO model predicts that essentially all of the oscillator strength is carried by a single transition that is predominantly HOMO → LUMO in character. The ZINDO calculations also give a lower excited state with almost no oscillator strength, as do recent calculations employing the excited-state molecular dynamics/collective electronic oscillator formalism with the AM1 reference Hamiltonian.[19] Chrom 4 is calculated to have a weak lowest electronic transition that is dominated by the HOMO → LUMO+1 configuration, followed by two strong, nearly degenerate transitions that are both predominantly HOMO → LUMO but have significant amounts of other configurations mixed in. The transition dipole moments of these two higher transitions are parallel to within 2°, whereas the weak lower transition is polarized at a 28° angle to the strong ones. Chrom 2 has a weak HOMO → LUMO+1 transition considerably below a very strong transition that is nearly pure HOMO → LUMO, with an angle of 51° between the two transition dipoles; the next highest electronic state is essentially forbidden.

The three computational methods employed predict very different ground-state equilibrium geometries, particularly with regard to the twisting of the azulenic group about its single bond linker. All three methods predict almost identical twist angles for Chrom 2 and Chrom 4, but these angles vary from 5 to 6° by DFT to 31° by AM1 and 63° by MINDO3. These differences in geometry translate into large differences in the predicted electronic excitations. Table 3 summarizes the wavelengths and oscillator strengths calculated for the three lowest singlet excited states of Chrom 2 and Chrom 4 by ZINDO at the equilibrium geometries resulting from the two semiempirical methods. At the highly twisted geometries predicted by both of the semiempirical methods, the strong charge-transfer transition is considerably blue-shifted relative to experiment and to its calculated wavelength at the nearly planar DFT geometry. In addition, the observed large red shift of this transition on lengthening the conjugated chain from Chrom 4 to Chrom 2 is reproduced fairly well at the DFT geometry, whereas the semiempirical geometries incorrectly give a blue shift of the strong transition on going from Chrom 4 to Chrom 2.

Discussion

The $S_0 \rightarrow S_1$ transition of unsubstituted azulene in solution shows extensive Franck−Condon activity in several vibrational modes and spans the entire region from 700 to 450 nm.[20] This transition involves predominantly the HOMO → LUMO excitation.[21] In the simplest picture, coupling of azulene to an acceptor group having a low-energy LUMO should result in two electronic transitions, the original azulene-localized excitation and a charge-transfer transition from the azulene HOMO to the thiobarbituric acid LUMO. In reality, of course, the situation is much more complicated; because the conjugation nominally extends across the molecule, the actual molecular orbitals will be to some extent delocalized over both donor and acceptor groups, and the resulting transitions may not be so simply distinguished as locally excited or charge transfer. However, we would expect more than one electronic transition in the visible region of the spectrum. The long-wavelength absorption of unsubstituted azulene has an oscillator strength of only about

TABLE 2: ZINDO Calculated Electronic Excitations at DFT Geometry[a]

Chrom 2			Chrom 4			JTB		
λ, nm	*f*	CI coeff	λ, nm	*f*	CI coeff	λ, nm	*f*	CI coeff
662	0.034	H → L+1 0.64	587	0.043	H → L+1 0.63 H → L 0.21	515	0.0001	H−1 → L+1 0.57 H−1 → L 0.38
573	1.71	H → L 0.66	501	0.51	H → L 0.49 H−1 → L+2 0.32 H−1 → L+3 0.27	423	1.01	H → L 0.67
498	0.0001	H−2 → L+3 −0.55 H−2 → L+2 0.27 H−2 → L 0.27	500	0.39	H → L 0.42 H−1 → L+2 −0.37 H−1 → L+3 −0.31 H−1 → L −0.20	396	0.002	H−5 → L 0.45 H−5 → L+2 −0.34 H−6 → L+2 −0.21

[a] Abbreviations: *f* = oscillator strength, H = highest occupied molecular orbital, L = lowest unoccupied molecular orbital.

TABLE 3: ZINDO Calculated Electronic Excitations at Semiempirical Geometries

Chrom 2				Chrom 4			
AM1 geometry		MINDO3 geometry		AM1 geometry		MINDO3 geometry	
λ, nm	f	λ, nm	f	λ, nm	f	λ, nm	f
639	0.05	555	0.05	628	0.11	579	0.06
542	0.0005	516	0.0002	547	0.001	546	0.0002
492	1.37	404	0.34	506	0.53	438	0.21

0.01,[22] but mixing with the charge-transfer transition could increase its intensity considerably.

In both azulenic chromophores the Raman transitions corresponding to the most acceptor-localized modes, the C═O stretch and the band tentatively assigned as the C═C stretch of the linker to the acceptor group, lose intensity as the excitation is tuned to the red side of the absorption band. This would suggest that the longer wavelength side of the band is dominated by the azulene-localized transition whereas the absorbance at shorter wavelengths has more charge-transfer character. The absorption spectrum of azulene in solution has its origin near 700 nm and a broad maximum around 600 nm. Thus the idea that an azulene-localized transition contributes more to the red side of the band is more consistent for Chrom 4 than for Chrom 2. The much redder absorption maximum of Chrom 2 compared with Chrom 4, which has the same electron donor and acceptor groups and differs only in the conjugated linker, suggests that most of the oscillator strength is carried by significantly delocalized transitions and calls into question any arguments based on localized transitions.

These qualitative expectations and the striking wavelength dependence of the resonance Raman intensities provide a good argument in favor of multiple electronic transitions. The ZINDO calculations provide only partial qualitative support for this hypothesis. The ZINDO calculations do predict that both Chrom 2 and Chrom 4 have a predominantly azulenic transition (HOMO → LUMO+1, where both orbitals are localized on the azulenic moiety) at lower energy than the predominantly charge-transfer transition (HOMO → LUMO, where the LUMO is located mainly on the thiobarbituric acid acceptor group). In the case of Chrom 4 the charge-transfer transition is actually a nearly degenerate pair of transitions having molecular orbital coefficients of nearly equal magnitude but opposite sign. However, in both molecules the azulenic transition is predicted to be only slightly stronger than in azulene itself (the lowest transition of unsubstituted azulene is calculated at 586 nm with an oscillator strength of 0.023), whereas the charge-transfer transition is stronger by more than an order of magnitude. Although quantum-mechanical interferences between transitions with highly disparate oscillator strengths can cause dramatic wavelength dependences in resonance Raman intensities,[23,24] when the two states are this strongly overlapping we would expect the intensities to be dominated by the stronger transition. The ZINDO calculations on JTB also give a transition at lower energy than the strong charge-transfer state, but its oscillator strength is negligible; this is consistent with our empirical modeling results that found no evidence for contributions from more than one electronic transition.[16] It should be pointed out that the ZINDO method employed here involves many approximations. In particular, it does not include the presence of a polar and polarizable solvent environment, which may substantially alter the properties of charge-transfer transitions. The charge-transfer transitions of all three molecules are calculated higher in energy than observed, and the red shift accompanying solvation might lead to a greater degree of coupling to the azulenic transition. In addition, the calculated transition energies and oscillator strengths are quite sensitive to the molecular geometry, as demonstrated in Table 3.

The long-wavelength transition of azulene is in-plane short-axis polarized,[22] whereas the charge-transfer transition is expected to be polarized roughly along a line connecting the centers of the donor and acceptor groups. The angle between these two vectors is fairly large for both Chrom 2 and Chrom 4 in any reasonable geometry, so if an azulene-localized transition and a charge-transfer transition were simultaneously contributing to the intensity of any Raman line, that line should exhibit a depolarization ratio different from 1/3 (the expected value for a single, nondegenerate electronic transition). Our observation that $\rho \approx 1/3$ for all lines does not, however, necessarily mean that a single electronic transition contributes. Depolarization ratios near 1/3 could arise from two different electronic transitions that enhance different sets of Raman modes, such that each Raman line draws most of its intensity from a single electronic transition. Depolarization ratios near 1/3 would also result from two electronic transitions that have nearly parallel transition dipole moments, although this is not supported by the ZINDO calculations, which predict fairly large angles between the two transition dipoles.

Other explanations for the striking relative Raman intensity variations across the absorption band cannot be ruled out. One possibility is that excitation in different parts of the absorption band selectively enhances different subsets of the molecular population that might differ, for example, in local solvation structure and/or molecular conformation (torsional angles). There is no obvious reason to expect particularly strong inhomogeneity for these chromophores in CH_2Cl_2 compared with other push−pull molecules in more strongly interacting solvents, where no such anomalies are observed.[9,16,25−27] However, the apparent excitation wavelength dependence of the frequencies of the oddly behaved transitions in Chrom 2 suggests some ground-state heterogeneity.[28−30] A strong dependence of the electronic transition moment on vibrational coordinate can also produce odd intensity patterns. In the Herzberg−Teller formulation of vibronic coupling, coordinate dependence of the electronic transition moment results from mixing of the various zero-order electronic states by a vibration, and so in a sense this is also a manifestation of contributions from more than one electronic state to the optical transition.

Conclusions

These experiments were initiated with the hope of understanding why the Kramers−Kronig based procedure for calculating hyperpolarizability dispersions from linear absorption spectra gives such poor results for Chrom 2.[10] The results suggest a fundamental breakdown of the two-electronic-state model as a reason for this failure. The Raman data also suggest that the hyperpolarizability dispersion of Chrom 4 should not be adequately described by a two-state model either, although the data for this molecule are not available. JTB, on the other hand, appears to behave as a reasonable two-electronic-state molecule from the standpoint of its linear absorption and resonance Raman spectra. It is hoped that the HRS or EFISH data needed for these theoretical relationships between linear absorption spectra and hyperpolarizability dispersions will become available for JTB or other likely candidates for true two-state behavior.

Acknowledgment. This work was supported in part by NSF grant CHE-0109920 and ONR grant N00014-02-1-0584 to A.M.K. C.H.W. acknowledges a 2001−2002 Guggenheim

Fellowship and a Big 12 Faculty Fellowship for support of this collaboration. We thank Professor Robert S. H. Liu for helpful discussions on the azulenic donor−acceptor chromophores.

References and Notes

(1) Prasad, P. N.; Williams, D. J. *Introduction to Nonlinear Optical Effects in Molecules and Polymers*; Wiley: New York, 1991.

(2) *Molecular Nonlinear Optics*: *Materials, Physics, and Devices*, Zyss, J., Ed.; Academic Press: Boston, 1993.

(3) *Nonlinear Optical Effects and Materials*, Günter, P., Ed.; Springer-Verlag: Berlin Heidelberg New York, 2000.

(4) Willetts, A.; Rice, J. E.; Burland, D. M.; Shelton, D. P. *J. Chem. Phys.* **1992**, *97*, 7590−7599.

(5) Orr, B. J.; Ward, J. F. *Mol. Phys.* **1971**, *20*, 513−526.

(6) Oudar, J. L.; Chemla, D. S. *J. Chem. Phys.* **1977**, *66*, 2664−2668.

(7) Wang, C. H. *J. Chem. Phys.* **2000**, *112*, 1917−1924.

(8) Berkovic, G.; Meshulam, G.; Kotler, Z. *J. Chem. Phys.* **2000**, *112*, 3997−4003.

(9) Moran, A. M.; Egolf, D. S.; Blanchard-Desce, M.; Kelley, A. M. *J. Chem. Phys.* **2002**, *116*, 2542−2555.

(10) Kelley, A. M. *J. Opt. Soc. Am. B* **2002**, *19*, 1890−1900.

(11) Hsu, C.-C.; Liu, S.; Wang, C. C.; Wang, C. H. *J. Chem. Phys.* **2001**, *114*, 7103−7108.

(12) Otomo, A.; Jäger, M.; Stegeman, G. I.; Flipse, M. C.; Diemeer, M. *Appl. Phys. Lett.* **1996**, *69*, 1991−1993.

(13) Myers, A. B.; Mathies, R. A. In *Biological Applications of Raman Spectroscopy*, Spiro, T. G., Ed.; Wiley: New York, 1987; Vol. 2, pp 1−58.

(14) Myers, A. B. In *Laser Techniques in Chemistry*, Myers, A. B., Rizzo, T. R., Eds.; Wiley: New York, 1995; pp 325−384.

(15) Woodford, J. N.; Wang, C. H.; Asato, A. E.; Liu, R. S. H. *J. Chem. Phys.* **1999**, *111*, 4621−4628.

(16) Moran, A. M.; Delbecque, C.; Kelley, A. M. *J. Phys. Chem. A* **2001**, *105*, 10208−10219.

(17) Frisch, M. J.; Trucks, G. W.; Schlegel, H. B.; Scuseria, G. E.; Robb, M. A.; Cheeseman, J. R.; Zakrzewski, V. G.; Montgomery, J. A., Jr.; Stratmann, R. E.; Burant, J. C.; Dapprich, S.; Millam, J. M.; Daniels, A. D.; Kudin, K. N.; Strain, M. C.; Farkas, O.; Tomasi, J.; Barone, V.; Cossi, M.; Cammi, R.; Mennucci, B.; Pomelli, C.; Adamo, C.; Clifford, S.; Ochterski, J.; Petersson, G. A.; Ayala, P. Y.; Cui, Q.; Morokuma, K.; Malick, D. K.; Rabuck, A. D.; Raghavachari, K.; Foresman, J. B.; Cioslowski, J.; Ortiz, J. V.; Baboul, A. G.; Stefanov, B. B.; Liu, G.; Liashenko, A.; Piskorz, P.; Komaromi, I.; Gomperts, R.; Martin, R. L.; Fox, D. J.; Keith, T.; Al-Laham, M. A.; Peng, C. Y.; Nanayakkara, A.; Gonzalez, C.; Challacombe, M.; Gill, P. M. W.; Johnson, B.; Chen, W.; Wong, M. W.; Andres, J. L.; Gonzalez, C.; Head-Gordon, M.; Replogle, E. S.; Pople, J. A. *Gaussian98*, revision A.7; Gaussian, Inc.: Pittsburgh, PA, 1998.

(18) Martin, J. M. L.; El-Yazal, J.; Francois, J.-P. *J. Phys. Chem.* **1996**, *100*, 15358−15367.

(19) Moran, A. M.; Kelley, A. M.; Tretiak, S. *Chem. Phys. Lett.*, submitted for publication.

(20) Klessinger, M.; Michl, J. *Excited States and Photochemistry of Organic Molecules*; VCH Publishers: New York, 1995.

(21) Negri, F.; Zgierski, M. Z. *J. Chem. Phys.* **1993**, *99*, 4318−4326.

(22) Small, G. J.; Kusserow, S. *J. Chem. Phys.* **1974**, *60*, 1558−1563.

(23) Phillips, D. L.; Myers, A. B. *J. Chem. Phys.* **1991**, *95*, 226−243.

(24) Markel, F.; Myers, A. B. *J. Chem. Phys.* **1993**, *98*, 21−30.

(25) Moran, A. M.; Bartholomew, G. P.; Bazan, G. C.; Kelley, A. M. *J. Phys. Chem. A* **2002**, *106*, 4928−4937.

(26) Moran, A. M.; Blanchard-Desce, M.; Kelley, A. M. *Chem. Phys. Lett.* **2002**, *358*, 320−327.

(27) Moran, A. M.; Kelley, A. M. *J. Chem. Phys.* **2001**, *115*, 912−924.

(28) Yamaguchi, T.; Kimura, Y.; Hirota, N. *J. Chem. Phys.* **1998**, *109*, 9075−9083.

(29) Yamaguchi, T.; Kimura, Y.; Hirota, N. *J. Chem. Phys.* **1998**, *109*, 9084−9095.

(30) Terenziani, F.; Painelli, A.; Comoretto, D. *J. Phys. Chem. A* **2000**, *104*, 11049−11054.